Modelling forest fires. Part II: reduction to two-dimensional models and simulation of propagation

J. Margerit, O. Séro-Guillaume *

LEMTA UMR 7563, 2 Avenue de la Forêt de Haye, 54504 Vandoeuvre les Nancy, France

Received 24 March 2001; received in revised form 2 July 2001

Abstract

This is the continuation of the paper named part I, where a three-dimensional model of combustion for forest fires has been derived. In this study the link between two-dimensional reaction diffusion models of propagation and three-dimensional combustion modelling is examined. By the way of an asymptotic analysis with the ratio of the height of vegetation to a characteristic size of the forest as small parameter, it is shown that two-dimensional models can be considered as inner expansion of general models. A hierarchy of three models is obtained and the simplest, which cope with drying, pyrolysis, wind and slope is simulated. Some of the features of real fires are obtained with this simplified model. © 2002 Elsevier Science Ltd. All rights reserved.

1. Introduction

In the paper [20] designated as part I we have derived a complete set of equations for the propagation of forest fires. To be useful this model need to be solved numerically. But first let us quickly recall the different approaches for modelling forest fires. Roughly speaking one can separate them in: cellular automata, envelop model, semi-empirical models, physical models. The following description is partly inspired from the one of Weber [26].

The cellular automata models [1,6,9,13,22], consist in modelling the forest as a set of nodes on a generally square lattice. The nodes can be in three states: unburned, burning or burnt. A probabilistic transition law involving the state of the node and the states of the neighbouring nodes governs the evolution of the automata. With these kind of models, which have simple rules, and give fast computation, one can introduce the interesting concept of percolation. Above the critical

occupation density the fire propagates to infinity, under this value the fire will extinguished. The critical density is an index of danger, which is a very useful information. However these models cannot produce genuine quantitative simulations, and there is no tentative to rely the transition law on some physical parameters defining the state of the forest.

The envelop model [16–18,21] is a geometrical model depending on three parameters. This model relies on the following ideas, under the action of wind and slope in a uniform forest, the front fire, coming from a source point, propagates as an ellipsis. Then between time t and $t + \mathrm{d}t$, all point of the fire front are source points and the fire front at time $t + \mathrm{d}t$ is the envelop of all these ellipses. Once the parameters have been fitted, this model produce realistic scenarios of propagation. It fails to work, if the fire front enclosed a non-convex domain. And here again there is no relation between the geometrical parameters and the physical balance laws and physical parameters of the forest.

The semi-empirical models, see [5,19] relies on correlation obtained in the laboratory added to a more or less simplified local balance of energy. They give a relatively fast computation, and estimate the propagation and the intensity of fires. Up to now there is no similarity rules for forest fire, which means that it is difficult to infer experimental results if the range of parameters

* Corresponding author. Tel.: +33-383-595604; fax: +33-383-595531.

E-mail address: osero@mailhost.ensem.u-nancy.fr (O. Séro-Guillaume).

Nomenclature

d	occupation density, dimensionless
$\mathbf{J}$	flux of mass diffusion, kg m^{-2} s^{-1}
K^{jk}	internal mass transfer from phase j toward phase k, kg m^{-3} s^{-1}
L	spectral intensity, W m^{-3} sr^{-1}
P	pressure, Pa
$\mathbf{Q}$	heat flux, W m^{-2}
Q_i	puissance produced by chemical reaction number i, W kg^{-1}
R_c	chemical reaction source term, W m^{-3}
Sa	saturation of solid or fluid elements, dimensionless
T	temperature, K
$\mathbf{V}$	velocity, m s^{-1}
W	molar mass, kg kmol^{-1}
X^{jk}	puissance transfer from phase j toward phase k, W m^{-3}
Y	mass fraction, dimensionless

Greek symbols

$\mathscr{E}^{\mathrm{p}}$	porosity of the wood as a porous medium, dimensionless
κ	permeability tensor, m^2
ρ	mass density, kg m^{-3}
$\mathscr{S}$	total stress tensor, N m^{-2}
$\mathscr{T}$	viscous stress tensor, N m^{-2}
Φ	porosity of the vegetal phase in the particle of vegetation, dimensionless
ψ	rate of mole production, kmol m^{-3} s^{-1}
$\dot{\omega}_i$	rate of mass production of the species number i, kg m^{-3} s^{-1}
Ω	space region

Superscript

$-$	variable above the vegetation layer

Subscripts

c	char
F	gaseous fuel
f	fluid phase
g	gas in porous vegetal
i	ith gas species
j, k	generic subscripts for gas or porous phase
l	liquid (water)
O	oxygen
R	residues of combustion
p	porous phase (vegetal)
r	radiation term
s	solid phase
T	tar
v	vapour
w	wood
_	variable under the vegetation layer

is not exactly the one involved in laboratory experiments.

All the preceding modelling fall in the class of "propagation models", as they aim to predict the position of the front flame.

The equations in physical models relies on the balance laws of physics. Some of these models are "postulated". Generally a two-dimensional system of reaction diffusion equations modelling the main processes is written [15,23,25] and the numerical simulations of these models are tractable. Another class of modelling has appeared that we could call "complete physical models" [10,12,20]. They aim to describe as faithfully as possible the combustion of vegetation. The vegetal fuel is described as an equivalent continuous medium. The system of equations for these models is much more complex by the number of processes described and also because they are three dimensional. The model that we derive in the part I belongs to this combustion model class. The question of the numerical simulation of such models is not yet resolved, the size of the corresponding codes should be of the same order than those of meteorology. Of course, the numerical simulation of such models will provide to firemen the needed information as the position of the fire front. So as to perform

tractable simulations, such complete physical models should be reduced.

In this paper we will try to relate complete physical models to two dimension reaction diffusion models. The main idea is that at a certain length scale L (distance from the fire front, size of a developed fire) the height of the vegetation δ is such that the ratio $\delta/L = \varepsilon$ is a small parameter, and the vegetation appears as a boundary layer. Indeed one can proceed to an asymptotic expansion using matched asymptotic expansion technique. The expansion inside the vegetation appears as the inner expansion, while the expansion outside the vegetation is the outer expansion. We will derive the inner expansion and consider the outer expansion as a parameter, in order to obtain a hierarchy of two-dimensional models. The models that we obtain are essentially reaction diffusion models. The simplest model is then simulated, it seems to capture some of the features of a real fire. This paper is structured as follows: Section 2 is devoted to the presentation of the three-dimensional models. In Section 3, the expansion is made and three reduced possible models are obtained with an increasing order of complexity. Section 4 is devoted to the simulation of the model number one obtained in Section 3.

## 2. Three-dimensional model of combustion in the vegetal stratum

2.1. Forest fire description

In the part I, we have proposed a complete three-dimensional combustion model, where the whole forest, i.e., vegetation and gases, occupies a stratum and is described as an equivalent medium at macroscopic level. The assumptions for deriving this model were the following: The forest at the *mesoscopic* scale can be considered as a porous medium, with porosity Φ. This porous medium, called vegetal phase, is composed of two phases: the first phase is the vegetation or p-phase (i.e., trunks, branches, twigs, leaves ...), denoted by index p and the second phase is a gaseous phase, or f-phase, denoted by index f, containing steam air and gases obtained after pyrolysis and combustion. One can consider that the main process in forest fire are heat transfer by radiation and convection, and the hydrodynamics of gas which allows to bring the oxygen necessary to the combustion and that the main effects of this heat transfer are drying of the vegetation, vegetation pyrolysis and pyrolysis flammable gases combustion that produce heat. This leads to forest fire propagation. (see Fig. 1 for the definition of the different scales and processes).

The p-phase, considered itself as a porous medium is constituted of a solid component with index s, a liquid component (water) denoted by the index l, and a gas constituent made of flammable gas denoted by the index F, steam denoted by the index v. The mass density of this gaseous phase is denoted by ρ_{g_p}, and the mass fraction of the gaseous species i is denoted by Y_{ig_p}. The porosity of the p-phase is $\mathscr{E}^p$.

Among solid constituents of the p-phase there are cellulose, hemicellulose and lignin. For sake of simplicity we group the above constituent as lumped "wood" species denoted by the index w and its mass densities is ρ_{w_p}. Wood will be decomposed during pyrolysis in flammable gas and char denoted by index c, with mass density is ρ_{c_p}. The model of pyrolysis reaction is a one step model:

$$\text{Cellulose} \xrightarrow{k} \text{Volatile fuel} + \text{Char}.$$
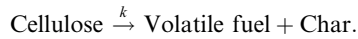
The symbols Sa_{w_p}, Sa_{c_p} will denote the saturation of solid species in the solid phase, while Sa_{g_p} and Sa_{l_p} will be the saturation of gaseous and liquid phases in vegetal phase.

The f-phase is a gaseous phase composed of oxygen, nitrogen, flammable gases, steam and residues of combustion. The mass density of this phase is denoted by ρ_f, and the mass fraction of the species j by Y_{jf}.

We have simplified the general model in part I in order to obtain the following system of equations that we summarise in the following sections.

2.2. Equations in the p-phase

The balance of energy or thermal equation is

$$(1 - \Phi)\rho_p C_P^p \frac{\partial T_p}{\partial t} = \nabla \cdot (\lambda_p \nabla T_p - \mathbf{Q}_{pr}) + R_{cp} + \chi(T_f - T_p). \tag{1}$$
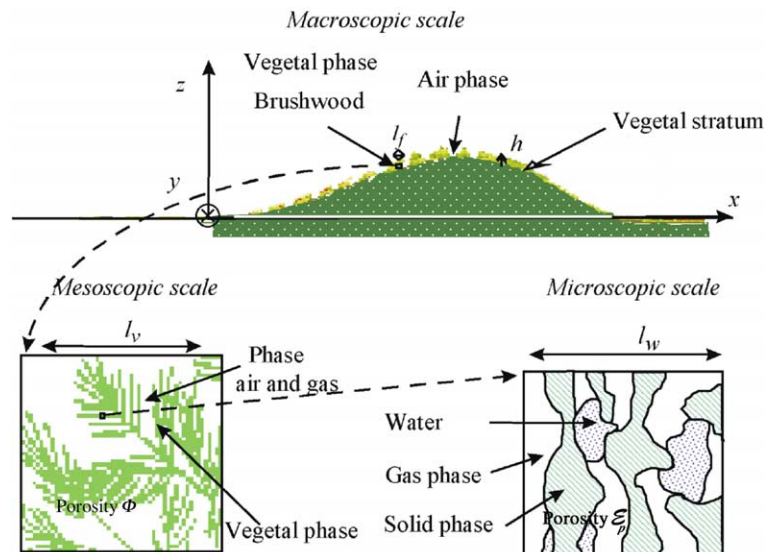

Fig. 1. Link between macroscopic, mesoscopic and microscopic scales.

The quantities in Eq. (1) have the following meaning: T_p is the temperature of the vegetal phase, ρ_p is the mass density of the vegetal phase and Φ is the mesoscopic porosity, λ_p is the equivalent heat conductivity and $\mathbf{Q}_{pr}$ is the heat released by radiation.

The heat capacity is defined by:

$$C_P^p = (1 - \mathscr{E}^p)\left(\mathrm{Sa}_{w_p}\frac{\rho_{w_p}}{\rho_p}C_{Pw_p} + \mathrm{Sa}_{c_p}\frac{\rho_{c_p}}{\rho_p}C_{Pc_p}\right)$$
$$+ \mathscr{E}^p\left(\mathrm{Sa}_{g_p}\frac{\rho_{g_p}}{\rho_p}\sum_i Y_{ig_p}C_{Pig_p} + \mathrm{Sa}_{l_p}\frac{\rho_{l_p}}{\rho_p}C_{Pl_p}\right) \quad (2)$$

with C_{Pi_j} the mesoscopic heat capacities. The chemical heat source is given by:

$$R_{cp} = -(1 - \mathscr{E}^p)(\mathrm{Sa}_{w_p}\rho_{w_p}Q_{w_p} + \mathrm{Sa}_{l_p}\rho_{l_p}Q_v), \quad (3)$$

where Q_{w_p} is the heat involved in pyrolysis and Q_v is the one produced by water vaporisation.

The balance of mass are for the cellulose

$$\frac{\partial}{\partial t}\left((1 - \Phi)(1 - \mathscr{E}^p)\mathrm{Sa}_{w_p}\right)$$
$$= -(1 - \Phi)(1 - \mathscr{E}^p)\mathrm{Sa}_{w_p}k_{w_pc_p}(T_p), \quad (4)$$

and for the char

$$\frac{\partial}{\partial t}\left((1 - \Phi)(1 - \mathscr{E}^p)\mathrm{Sa}_{c_p}\rho_{c_p}\right)$$
$$= (1 - \Phi)(1 - \mathscr{E}^p)\mathrm{Sa}_{w_p}\rho_{w_p}k_{w_pc_p}(T_p), \quad (5)$$

where the functions k_i and k_{i_j} are phenomenological functions that follow Arrhenius type laws.

For the liquid phase

$$\frac{\partial}{\partial t}\left((1 - \Phi)(\mathscr{E}^p\mathrm{Sa}_{l_p})\right) = -(1 - \Phi)\mathscr{E}^p\mathrm{Sa}_{l_p}k_{l_pv_{gp}}(T_p). \quad (6)$$

In the gaseous phase

$$\frac{\partial}{\partial t}\left((1 - \Phi)\mathscr{E}^p\mathrm{Sa}_{g_p}\rho_{g_p}Y_{i_{gp}}\right)$$
$$= -(1 - \Phi)(1 - \mathscr{E}^p)k_{w_pF_{gp}}(T_p)\mathrm{Sa}_{w_p} - K_{F_{gp}}^{pf}, \quad (7)$$

and for the mass fraction of flammable gases

$$\frac{\partial}{\partial t}\left((1 - \Phi)\mathscr{E}^p\mathrm{Sa}_{g_p}\rho_{g_p}Y_{v_{gp}}\right)$$
$$= (1 - \Phi)\mathscr{E}^p k_{l_pv_{gp}}(T_p)\mathrm{Sa}_{l_p}\rho_{l_p} - K_{v_{gp}}^{pf}. \quad (8)$$

The functions $K_{ig_p}^{pf}$, for $i = v, F$, correspond to the outflow of gases from the p-phase to the f-phase. The densities ρ_{w_p}, ρ_{c_p}, and ρ_{l_p} can be considered as constant.

2.3. Equations in the fluid f-phase

The energy balance is

$$\Phi\rho_f C_P^f\left(\frac{\partial T_f}{\partial t} + \mathbf{V}_f \cdot \nabla T_f\right)$$
$$= \nabla \cdot [\lambda_f \nabla \cdot T_f - \mathbf{Q}_{rf}] + R_{cf} - \chi(T_f - T_p), \quad (9)$$

where $\mathbf{Q}_{rf}$ is the heat released by radiation. The chemical heat source is a function of temperature and of the mass fractions of gases involved in combustion reaction, that is $R_{cf} = Q_{cf}\psi(T_f)$ with $\psi = k(T_f)(\rho_f Y_{Ff})^{v_F}(\rho_f Y_{Of})^{v_O}$. The heat capacity is given by $C_{Pf} = \sum_i Y_{if}C_{Pi}$.

The balance of momentum is

$$\Phi\rho_f\left(\frac{\partial \mathbf{V}_f}{\partial t} + \nabla\mathbf{V}_f \cdot \mathbf{V}_f\right)$$
$$= -\Phi\nabla P_f + \Phi\rho_f\mathbf{g} + \nabla(\lambda\nabla \cdot \mathbf{V}_f)$$
$$+ \left(K^{pf}\mathbf{Id} - \eta\Phi^2\kappa\right)\mathbf{V}_f + \mu\Delta\mathbf{V}_f, \quad (10)$$

where λ and μ are the two viscosities of the equivalent fluid, while η is the viscosity at microscopic level, κ^{-1} is the drag tensor, $\mathbf{Id}$ is the identity tensor, $\mathbf{g}$ is the gravity and $K^{pf} = \sum_i K_i^{pf}$ is the total outflow of gases from p-phase to f-phase.

The balances of mass equations can be written generically

$$\frac{\partial}{\partial t}(\Phi\rho_f Y_{if}) + \nabla \cdot (\Phi\rho_f Y_{if}\mathbf{V}_f + \mathbf{J}_{if})$$
$$= \Phi\dot{\omega}_i + K_{ig_p}^{pf} \quad \text{for } i = F, O_2, N_2, v, P, \quad (11)$$

with $\dot{\omega}_j = -v_j W_j\psi(T_f, Y_F, Y_{O_2}), \dot{\omega}_P = v_P W_P\psi(T_f, Y_F, Y_{O_2})$, and $\dot{\omega}_{N_2} = \dot{\omega}_v = 0$. Moreover the outflows $K_{ig_p}^{pf}$ are given by the following relations:

$$\tau_i\frac{\partial K_{ig_p}^{pf}}{\partial t} + K_{ig_p}^{pf} = k_i^{pf}(T_p)l(Y_{ig_p}, Y_{if}) \quad \text{for } i = F, v \quad (12)$$

and $K_{ig_p}^{pf} = 0$ for $i = O_2, N_2, R$. The usual thermodynamics relation is also verified:

$$P_f = \rho_f RT_f\sum_i Y_{if}/W_i. \quad (13)$$

2.4. Boundary conditions

As indicated in part I, the equivalent medium has been obtained by averaging the mesoscopic quantities with a smooth kernel with compact support. The quantities associated to the p-phase are defined inside the domain Ω occupied by this phase, see Fig. 2 for the definition of this domain. While quantities associated to the f-phase can be extended to the domain outside the vegetation, provide the parameters in relations Eqs. (9)–(14) are supposed to depend on co-ordinates, for example the porosity is Φ inside the vegetation and 1 outside, but because of the smoothing effect of the kernel the porosity decreased rapidly but remains smooth. Therefore the boundary conditions for the p-phase are natural conditions while boundary conditions for the f-phase at the interface between domain Ω and the atmosphere are unnatural, they only indicate continuity of quantities.
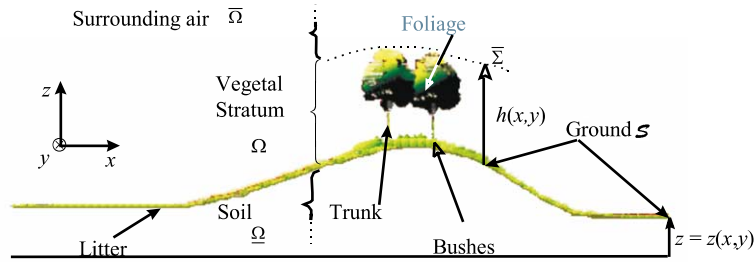
Fig. 2. Strata positions in the vegetation.

The boundary conditions at the interfaces between vegetation and surrounding atmosphere, denoted by $\bar{\Sigma}$, and vegetation-soil denoted by $\underline{\Sigma}$ for the p-phase are:

$$-\lambda_p \nabla T_p \cdot \mathbf{n} = h_L(T_p - T_e) + M_r \quad \text{on } \bar{\Sigma}, \tag{14}$$

$$\nabla T_p \cdot \mathbf{n} = 0 \quad \text{on } \underline{\Sigma}, \tag{15}$$

where M_r is the radiation heat flux from the flames above the vegetation.

The boundary conditions for the f-phase are:

$$\nabla T_f \cdot \mathbf{n} = 0 \quad \text{on } \underline{\Sigma}, \tag{16}$$

$$\mathbf{V}_f = 0 \quad \text{on } \underline{\Sigma}. \tag{17}$$

We must consider only that the quantities are continuous across the upper interface $\bar{\Sigma}$. The temperature T_e in Eq. (14) is the temperature of gases in the upper domain, but as the temperature is continuous across the interface, it is equal to the temperature in the f-phase. More complex interface conditions between the vegetal phase and the atmosphere could be used. But it seems that, due to the size of the elementary representative volume, the boundary layer due to the presence of the interface is not so important. At the very end, the choice of these conditions has no real importance here because we will not match the outer and inner expansions in the asymptotic expansion of the next section.

3. Reduction to two-dimensional modelling

Let us consider that the height scale of the vegetal stratum is δ, so that the equation for the upper part of the vegetation can be written $z = \delta h(x, y)$ with $h \leqslant 1$, see Fig. 2. We can consider now a "gigascopic" scale L associated to a developed fire or corresponding to a distance from the flames front such that the ratio δ/L is a small parameter say ε. At scale L, vegetation appears as a boundary layer and the fire can be considered as spreading on a surface. We can put the system of equations in non-dimensional form using L as length scale, i.e., we consider the new co-ordinate $\bar{\mathbf{x}} = \mathbf{x}/L$, temperatures $\bar{T}_j = (T_j - T_a)/T_a$ for $j = p, f$. The temperature T_a is an equilibrium temperature far from the front flames. The unit time is the time for a cubic cell of size δ to ignite under the heat flux M_r, that is

$$\bar{t} = t \frac{M_r}{(1 - \Phi)\tilde{\rho}_p \tilde{C}_{P_p}(T_i - T_a)\delta},$$

$\tilde{\rho}_p$ and $\tilde{C}_{P_p}$ are relevant average values for the mass density and the heat capacity. There is no relevant characteristic scale for the velocity of gases, but we could introduce the velocity of the gases far from the front flame above vegetation. This velocity is mainly horizontal. We will not rewrite all the system of equations with these new variables, and will keep the same notations as previously. For sake of simplicity we suppose that the ground is horizontal and that the height of the vegetation is constant, that is $h(x, y) = 1$ so that the domain Ω is defined by $-\infty < x, y < \infty, 0 < z < \delta/L = \varepsilon$. Let us consider an asymptotic expansion of the preceding system of equation, we introduce two new fast variables:

$$z_1 = z/\varepsilon, \quad t_1 = t/\varepsilon^2, \tag{18}$$

all quantities will be expanded as:

$$f = f_0(x, y; t; z_1, t_1) + \varepsilon f_1(x, y, t; z_1, t_1) + \varepsilon^2 f_2(x, y, t; z_1, t_1) + \cdots \tag{19}$$

For doing the expansion, the following hypothesis will be used:

(a) The vertical component w of the velocity will be supposed such that $w = O(\varepsilon)$, i.e., $w_0 = 0$, it is nothing but the fact that velocity is mainly horizontal in this region.

(b) The temperature T_p and T_f are of the same order, at least at the upper interface of the domain.

(c) The external radiative heat flux M_r is of order ε.

Hypothesis (b) can be justified by the fact that in the upper part of the vegetal stratum, the vegetation size is small and the contact surface between the two phases is important so that a "relative" thermal equilibrium can occur.

The expansion will be a multiple scale expansion in time for the two phases and an inner expansion (in the sense of matched asymptotic expansion) in the vertical co-ordinate for the f-phase.

We will detail the calculations only for the thermal equations in the two phases.

3.1. Expansion in the p-phase

For expanding Eq. (1) one must replace

$$\frac{\partial}{\partial t} \to \frac{1}{\varepsilon^2}\frac{\partial}{\partial t_1} \quad \text{and} \quad \frac{\partial}{\partial z} \to \frac{1}{\varepsilon}\frac{\partial}{\partial z_1},$$

multiplying by ε^2 one obtains the cascade of equations:
Order 1 (ε^0):

$$(1-\Phi)\rho_{p0}C_{P0}^p \frac{\partial T_{p0}}{\partial t_1} = \lambda_{p0}\frac{\partial^2 T_{p0}}{\partial z_1^2} \quad \text{for } 0 < z_1 < 1, \qquad (20)$$

$$\frac{\partial T_{p0}}{\partial z_1} = 0 \quad \text{for } z_1 = 1, \qquad (21)$$

$$\frac{\partial T_{p0}}{\partial z_1} = 0 \quad \text{for } w = O(\varepsilon), \qquad (22)$$

where ρ_{p0} is put for $\rho_p(T_{p0})$, for example. The solution of Eqs. (20)–(22) is the sum of a function of t_1, z_1 which tends to zero on the timescale ε^2 and of an unknown function of x, y, t that we denote by $T_{p0}(x, y, t)$.
Order 2 (ε^1):

$$(1-\Phi)\rho_{p0}C_{P0}^p \frac{\partial T_{p1}}{\partial t_1} = \lambda_{p0}\frac{\partial^2 T_{p1}}{\partial z_1^2} - \frac{\partial Q_{rp3}}{\partial z_1} \quad \text{for } 0 < z_1 < 1,$$

$$\frac{\partial T_{p1}}{\partial z_1} = 0 \quad \text{for } z_1 = 1,$$

$$\frac{\partial T_{p1}}{\partial z_1} = 0 \quad \text{for } z_1 = 0.$$

The expansion at order 3 (ε^2) gives the equation:

$$(1-\Phi)\rho_{p0}C_{P0}^p \frac{\partial T_{p2}}{\partial t_1}$$
$$= \lambda_{p0}\frac{\partial^2 T_{p2}}{\partial z_1^2} + \left(-\rho_{p0}C_{Pp0}\frac{\partial T_{p0}}{\partial t} + \lambda_{p0}\Delta_S T_{p0} \right.$$
$$\left. -\nabla_S \cdot \mathbf{Q}_{rp0} + R_{cp0} + \chi(T_{f0} - T_{p0}) \right)$$
$$\text{for } 0 < z_1 < 1 \qquad (23)$$

$$\lambda_{p0}\frac{\partial T_{p2}}{\partial z_1} = h_L(T_{p0} - T_{f0}) + M_r \quad \text{for } z_1 = 1, \qquad (24)$$

$$\frac{\partial T_{p2}}{\partial z_1} = 0 \quad \text{for } z_1 = 0. \qquad (25)$$

We have kept at this order the exchange term between the two phases. Let us denote the term between parenthesis in the right-hand side of Eq. (23) by a, it is a constant with respect to fast variables. In the multiple scales expansion the function T_{p2} must be bounded, the condition for this function to tend to a bounded limit when $t_1 \to \infty$ is that the system (23)–(25) has a stationary solution, so that the solution tends to this

limit. And the condition for this system to have a stationary solution is:

$$\int_0^1 \left(-(1-\Phi)\rho_{p0}C_{P0}^p\frac{\partial T_{p0}}{\partial t} + \lambda_{p0}\Delta_S T_{p0} - \nabla_S \cdot \mathbf{Q}_{rp0} + R_{cp0} \right.$$
$$\left. + \chi(T_{f0} - T_{p0}) \right) dz_1 = -\left[\lambda_{p0}\frac{\partial T_{p2}}{\partial z_1} \right]_0^1$$

which gives the compatibility condition:

$$(1-\Phi)\rho_{p0}C_{P0}^p\frac{\partial T_{p0}}{\partial t} = \lambda_{p0}\Delta_S T_{p0} - \nabla_S \cdot \mathbf{Q}_{rp0} + R_{cp0}$$
$$+ \chi'(T_{f0} - T_{p0}) + M_r, \qquad (26)$$

the operators involved in relation (26) are surface operators. This is a two-dimensional reaction diffusion relation. Let us notice that the quantities at this order can be approximated by their average on the stratum that is:

$$T_{p0} = \frac{1}{\varepsilon}\int_0^\varepsilon T_p(x, y, z, t)\,dz + O(\varepsilon).$$

The other equations for the mass balance are simply obtained because they do not involved operators with spatial derivative, so that asymptotic equations for Eqs. (4)–(8) provide quantities are replaced by their average on the stratum.

3.2. Expansion in the f-phase

The algebra is almost the same, but we must take into account now that the expansion is a multiple scale expansion in time but an inner expansion in z and that the boundary conditions are changed at the upper interface. Let us detail the calculus for the thermal equation (9).
Order 1 (ε^0):

$$\Phi\rho_{f0}C_{P0}^f\frac{\partial T_{f0}}{\partial t_1} = \lambda_{f0}\frac{\partial^2 T_{f0}}{\partial z_1^2} \quad \text{for } 0 < z_1 < 1, \qquad (27)$$

$$T_{f0} = f(x, y, t) \quad \text{for } z_1 = 1, \qquad (28)$$

$$\frac{\partial T_{f0}}{\partial z_1} = 0 \quad \text{for } z_1 = 0, \qquad (29)$$

where $f(x, y, t)$ is an unknown function. The solution of Eqs. (27) and (28) is the sum of a function of t_1, z_1 which tends to zero on the timescale ε^2 and of an unknown function of x, y, t that we denote by $T_{f0}(x, y, t)$.
Order 2 (ε^1):

$$\Phi\rho_{f0}C_{P0}^f\frac{\partial T_{f1}}{\partial t_1} = \lambda_{f0}\frac{\partial^2 T_{f1}}{\partial z_1^2} \quad \text{for } 0 < z_1 < 1,$$

$$T_{f1} = 0 \quad \text{for } z_1 = 1,$$

$$\frac{\partial T_{f1}}{\partial z_1} = 0 \quad \text{for } z_1 = 0.$$

Here we have neglected the radiation heat flux.

At order 3 (ε^2) we obtain the equation:

$$\Phi\rho_{f0}C_{P0}^f \frac{\partial T_{p2}}{\partial t_1}$$
$$= \lambda_{f0}\frac{\partial^2 T_{f2}}{\partial z_1^2} + \left(-\rho_{f0}\Phi C_{P0}^f \left(\frac{\partial T_{f0}}{\partial t} + \mathbf{V}_0 \cdot \nabla_S T_{f0}\right)\right.$$
$$\left. + \lambda_{f0}\Delta_S T_{f0} + R_{cf0} - \chi(T_{f0} - T_{p0})\right)$$

for $0 < z_1 < 1$, (30)

$$T_{f2} = 0 \quad \text{for } z_1 = 1,$$ (31)

$$\frac{\partial T_{p2}}{\partial z_1} = 0 \quad \text{for } z_1 = 0.$$ (32)

Let us denote the term between parenthesis in the right-hand side of Eq. (30) by a, it is a constant with respect to fast variables. The function T_{f2} can be written as the sum $v + v_1$, with:

$$\lambda_{f0}\frac{\partial^2 v_1}{\partial z_1^2} = -a, \quad v_1(z_1 = 0, t_1) = \frac{\partial v_1}{\partial z_1}(z_1 = 0, t_1) = 0,$$

and

$$\Phi\rho_{f0}C_{P0}^f \frac{\partial v}{\partial t_1} = \lambda_{f0}\frac{\partial^2 v}{\partial z_1^2},$$
$$v(z_1 = 0, t_1) = \frac{\partial v}{\partial z_1}(z_1 = 0, t_1) = 0, \quad v(z_1, 0)$$

given. v tends to 0 when $t_1 \to \infty$ and $v_1 = -(a/2\lambda_{f0})(z_1^2 - 1)$. But in order to match the expansion when $z_1 \to \infty$, T_{f2} must be bounded so that $a = 0$. And therefore the compatibility condition can be written:

$$\rho_{f0}\Phi C_{P0}^f \left(\frac{\partial T_{f0}}{\partial t} + \mathbf{V}_{f0} \cdot \nabla_S T_{f0}\right)$$
$$= \lambda_{f0}\Delta_S T_{f0} + R_{cf0} - \chi(T_{f0} - T_{p0}).$$ (33)

Here again we obtain a two-dimensional equation, set on the surface ground. The algebra is almost the same for the equations of mass balance and balance of momentum and we obtain the two-dimensional equations:

$$\frac{\partial}{\partial t}(\Phi\rho_{f0}Y_{if0}) + \nabla_S \cdot (\Phi\rho_{f0}Y_{if0}\mathbf{V}_{f0} + \mathbf{J}_{if0})$$
$$= \Phi\dot{\omega}_{i0} + K_{ig_p0}^{pf},$$ (34)

$$\Phi\rho_{f0}\left(\frac{\partial \mathbf{V}_{f0}}{\partial t} + \nabla_S \mathbf{V}_{f0} \cdot \mathbf{V}_{f0}\right)$$
$$= -\Phi\nabla_S P_{f0} + \nabla_S(\lambda\nabla_S \cdot \mathbf{V}_{f0}) + \left(K^{pf}\mathbf{Id}_2 - \eta\Phi^2\boldsymbol{\kappa}_2^{-1}\right)\mathbf{V}_{f0}$$
$$+ \mu\Delta_S\mathbf{V}_{f0}.$$ (35)

3.3. About the two-dimensional models of propagation

In fact we can consider this set of equations as a hierarchy of modelling with increasing complexity. The first model is just Eq. (26). The parameters of this equations i.e., ρ_{p0}, C_{P0}^p depend on the mass fraction of the constituent of the p-phase, but at first approximation we can neglect the influence of the gaseous phase in the p-phase and consider that they depend only on solid and liquid species. Therefore the model is the following (in the equations below and in the following we will suppress the index 0):

(i) Model I

$$(1-\Phi)\rho_p C_P^p \frac{\partial T_p}{\partial t} = \lambda_p\Delta_S T_p - \nabla_S \cdot \mathbf{Q}_{rp} + R_{cp}$$
$$+ \chi'(T_f - T_p) + M_r,$$ (26)

$$\frac{\partial}{\partial t}\left((1-\Phi)(1-\mathscr{E}^p)\mathrm{Sa}_{w_p}\right)$$
$$= -(1-\Phi)(1-\mathscr{E}^p)\mathrm{Sa}_{w_p}k_{w_p}(T_p),$$ (4)

$$\frac{\partial}{\partial t}\left((1-\Phi)(1-\mathscr{E}^p)\mathrm{Sa}_{c_p}\rho_{c_p}\right)$$
$$= (1-\Phi)(1-\mathscr{E}^p)\mathrm{Sa}_{w_p}\rho_{w_p}k_{w_p c_p}(T_p),$$ (5)

$$\frac{\partial}{\partial t}\left((1-\Phi)(\mathscr{E}^p\mathrm{Sa}_{l_p})\right) = -(1-\Phi)\mathscr{E}^p\mathrm{Sa}_{l_p}k_{l_p v_{gp}}(T_p)$$ (6)

with

$$C_P^p = (1-\mathscr{E}^p)\left(\mathrm{Sa}_{w_p}\frac{\rho_{w_p}}{\rho_p}C_{Pw_p} + \mathrm{Sa}_{c_p}\frac{\rho_{c_p}}{\rho_p}C_{Pc_p}\right)$$
$$+ \mathscr{E}^p\left(\mathrm{Sa}_{l_p}\frac{\rho_{l_p}}{\rho_p}C_{Pl_p}\right),$$

and the heat source R_{cp} is a known function of temperature.

As the functions involved in chemical kinetic are supposed to be given this system is in someway closed. The temperature T_f is the only internal parameter of the model. Of course, the radiative heat flux on $\bar{\Sigma}$ incorporates all the effect of the "outer expansion", i.e., of the processes which take place outside the vegetal stratum and it depends on external parameters as height and temperature of flames above vegetation ...

It should be desirable to calculate the temperature of the f-phase, then we must add Eq. (33) to model I. However the chemical heat source term in the preceding equation depend on the mass fractions of gases Y_{if}, so that we must add the equations for balance of mass (34) and the Eq. (12) for the outflows $K_{ig_p}^{pf}$.

Therefore the second model will be:

(ii) Model II

Equations of model I plus

$$\rho_f\Phi C_P^f\left(\frac{\partial T_f}{\partial t} + \mathbf{V}_f \cdot \nabla_S T_f\right) = \lambda_f\Delta_S T_f + R_{cf} - \chi(T_f - T_p),$$

(33)

$$\frac{\partial}{\partial t}(\Phi\rho_f Y_{if}) + \nabla_S \cdot (\Phi\rho_f Y_{if}\mathbf{V}_f + \mathbf{J}_{if}) = \Phi\dot{\omega}_i + K_{ig_p}^{pf}, \quad (34)$$

$$\tau_i \frac{\partial K_{ig_p}^{pf}}{\partial t} + K_{ig_p}^{pf} = k_i^{pf}(T_p)l(Y_{ig_p}, Y_{if}). \quad (12)$$

This model is closed (apart from the external quantities as for model I) provide that the velocity field $\mathbf{V}_f$ is given. Of course the velocity plays an important role in the propagation of fire because of the necessity to bring fresh air to combustion.

Model III is constituted of model II to which equation of balance of momentum is added:

(iii) Model III

Equations of model II plus

$$\Phi\rho_f\left(\frac{\partial\mathbf{V}_f}{\partial t} + \nabla_S\mathbf{V}_f \cdot \mathbf{V}_f\right)$$

$$= -\Phi\nabla_S P_f + \nabla_S(\lambda\nabla_S \cdot \mathbf{V}_f)$$

$$+ (K^{pf}\mathbf{Id}_2 - \eta\Phi^2\boldsymbol{\kappa}_2^{-1})\mathbf{V}_f + \mu\Delta_S\mathbf{V}_f. \quad (35)$$

For this model only quantities given by the outer expansion (i.e., external equations) are parameters. That is the only parameter of the model is the radiative heat flux M_r.

In part I we have considered the possibility for the two phase to be at thermal equilibrium, at least in a large part of the domain. In this case there a unique thermal equation (Eq. (101) of part I) and it is interesting to proceed to the same asymptotic expansion that we have previously done for the two temperatures model. One obtains the following model:

(iv) Model I′

$$\rho C_P \frac{\partial T}{\partial t} + \rho_f \Phi C_P^f \mathbf{V}_f \cdot \nabla_S T$$

$$= \lambda_{eq}\Delta_S T + R_c(T) + \nabla \cdot \mathbf{Q}_r + M_r + h(T_{ext} - T) \quad (36)$$

with $\rho C_P = (\Phi\rho_f C_P^f + (1 - \Phi)\rho_p C_P^p)$, T_{ext} is an external temperature associated to upper interface boundary condition. Eqs. (4)–(6) must be added to Eq. (36), with $T_p = T$. Of course in this modelling the combustion heat source R_c is not properly taken into account because it depends on the gaseous mass fractions.

Models I and I′ are reaction diffusion models resembling to the one proposed by Provatas et al. [14] or Weber [24,25]. Essential difference remains, they are considered as inner expansions of a three-dimensional model and they are coupled to the outer part of the expansion by at least two terms. The first one is the external temperature which cannot be considered as constant, the second one related to the first one is the non-local radiative heat flux M_r. The possibility of estimating these two terms remains unexplored and is closely related to the domain of validity of the expansion derived here. This expansion cannot be uniformly valid because close to the flame or inside it, the dominant term

in the thermal equations are the chemical heat sources and the vertical component of the velocity cannot be neglected, the phenomenon in this region should be essentially three dimensional.

4. Simulation of the simplest previous model

In this section we explore the consequence of model I that we derived in the preceding section. We will first neglect the internal radiation heat source $\mathbf{Q}_r$ versus the external radiation heat source M_r, see [2]. Let us analyse the chemical heat source. A typical thermo-gravimetric (TG) analysis law giving the loss mass of a piece of vegetation during heating as function of the temperature is given by Fig. 3.

If the activation energy is important the curve is very stiff. At first approximation we can consider that the loss mass is null before a certain temperature of pyrolysis and is a given temperature function after this value. The pyrolysis is a reaction weakly endothermic so that we can neglect Q_{w_p} in the chemical heat source. The region in the forest (the burning region) where the pyrolysis occurs is reduced to a curve, this curve can be considered as a first free boundary. This analysis is equivalent to say that the characteristic time for chemical reaction of pyrolysis is much smaller that the characteristic time of fire spreading. Moreover if we neglect the time of chemical reaction of combustion we can assume that the temperature of pyrolysis is also the temperature of ignition T_{ig}. The same kind of analysis can be made for the drying: there is no evaporation before a certain temperature T_{ev}. After this temperature the heat vaporisation is greater than the accumulation term $\rho_p C_P^p(\partial T_p/\partial t)$ in the left-hand side of the temperature equation, so that we can neglect it. As the front of pyrolysis and the front of drying are assumed to be sharp we can neglect heat
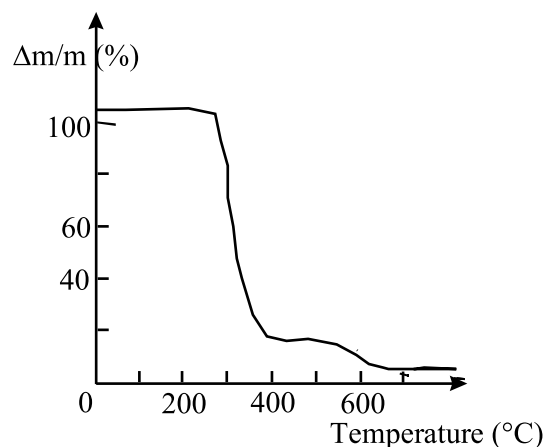

Fig. 3. Mass loss.

conduction in the vegetation. Therefore there is two free boundaries, the first is the fire front defined by an ignition temperature T_{ig}, and the second is the drying zone defined by an evaporation temperature T_{ev}. Now the heat source term M_r is produced by the flames above the surface neighbourhood, and we must evaluate this term.

4.1. The model

We can consider non-local radiation. The radiation transfer M_r is given by the product of convolution:

$$M_r(\mathbf{M}, t) = \int_\Omega \varphi(\mathbf{P}, t) \xi^*(\mathbf{P}, \mathbf{M}) \, d\omega \tag{37}$$

with:

$$\varphi(\mathbf{P}, t) = \delta h_f K(\mathbf{P}) \frac{B}{\pi} T^4(\mathbf{P}, t) \tag{38}$$

and

$$\xi(\mathbf{P}, \mathbf{M}) = \frac{K(\mathbf{P})}{\|\mathbf{MP}\|}$$
$$\times \exp\left(-K(\mathbf{P}) \frac{(1 + \sin^2 \alpha_f)(1 - \sin \alpha_f \cos(\varphi - \varphi_f))}{\cos^2 \alpha_f} \|\mathbf{MP}\| \right), \tag{39}$$

$K = \beta \sigma / 4$, is the extinction coefficient.

See Appendix A for the derivation of such simplified Eqs. (37)–(39) for radiation heat transfer.

We consider equation set (26) in dimensional form, taking into account the preceding assumptions. We denote H_u by the vegetation moisture, ρ_p by the load or the surface density of the vegetation, T by the temperature, the density lower bound of extinction is denoted by ρ_{ext}, it corresponds to the density of pyrolysis residues.

The system is the following:

(i) Before the fire font: $T \leqslant T_{ig}, H_u > 0$ and $\rho_p > \rho_{ext}$

$$(1 - \Phi)\rho_p(C_s + H_u C_l)\frac{\partial T}{\partial t} = M_r - h(T - T_a)$$

if $T < T_{ev}$,

$$-\rho_p L_{ev}\frac{\partial H_u}{\partial t} = M_r - h(T_{ev} - T_a) \tag{40}$$

if $T = T_{ev}$ and $H_u > 0$,

$$(1 - \Phi)\rho_p C_s \frac{\partial T}{\partial t} = M_r - h(T - T_a) \quad \text{if } T > T_{ev},$$

where C_s is the heat capacity of the solid constituent of vegetation, C_w is the heat capacity of the water; h is the heat loss coefficient, L_{ev} is an evaporation latent heat, T_a is the external temperature.

(ii) In the burning zone: $T > T_{ig}, H_u = 0$ and $\rho_p \geqslant \rho_{ext}$
The temperature is constant and equal to the ignition temperature:

$$T = T_{ig} \tag{41}$$

the variation of mass due to chemical reactions

$$\frac{\partial \rho_p}{\partial t}(\mathbf{P}, t) = v_r(\mathbf{P}, t - t_{ig})\rho_p(\mathbf{P}, t), \tag{42}$$

t_{ig} is the instant of ignition and v_r characterised the speed of the chemical reaction, one can consider an Arrhenius law:

$$v_r(\mathbf{P}, t - t_{ig}) = A \exp(-E/RT). \tag{43}$$

(iii) In the burnt zone: $T \leqslant T_{ig}$ and $\rho_p = \rho_{ext}$.

$$T = T_a. \tag{44}$$

The non-local term for the radiation term is principally similar to the one used by Dorrer [8], as almost model see Albini, Provatas, Weber it contains a cooling term, but we have neglected the conduction (or diffusion). This hypothesis is not a real defect, the corresponding effect could be included in future simulation, and it is consistent with the hypothesis of sharp front of drying and pyrolysis. The main difference is in the treatment of heat source term including the drying of vegetation.

5. Result of numerical simulations

5.1. General results of simulations

This section is devoted to the numerical simulation of model I (37)–(39). Before doing any numerical computation let us put the system on a non-dimensional form. We consider the characteristic time:

$$\tau = \frac{P_r C_p (T_{ig} - T_a)}{\delta h_f T_f^4 K_r^2}, \tag{45}$$

where P_r is the maximum load, K_r is a characteristic extinction coefficient. With the non-dimensional quantities:

$$r^* = \frac{r}{L}, \quad t^* = \frac{t}{\tau}, \quad T^* = \frac{T - T_a}{T_{ig} - T_a}, \quad P_p^* = \frac{P_p}{P_r}, \tag{46}$$

The star on the new variables has been omitted. The non-dimensionless parameters involved in the model are:

$$P_{ext} = P_{ext}/P_r, \quad L_{ev} = \frac{L_{ev}}{C_p(T_{ig} - T_a)},$$

$$h = \frac{(T - T_a)Kh}{h_f a^2 B T_f^4}, \quad C_w = \frac{C_w}{C_p}, \tag{47}$$

$$T_{ev} = \frac{T_{ev} - T_a}{T_{ig} - T_{ev}}, \quad v_g = \frac{V}{\sqrt{gh_f}}. \tag{48}$$

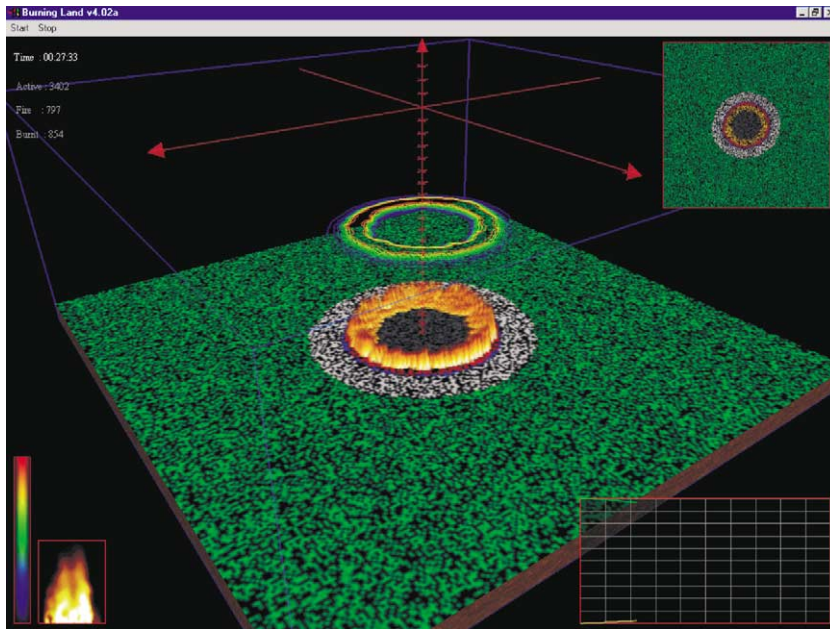If we consider the following values for the physical constants:

Fig. 4. Propagation of a fire $d = 0.5$, and humidity is 7%.

$C_P = 2400$ J/kg K	$\cos \alpha_f = 1$
$\delta = 1$ m	$K = \beta\sigma/4 = 0.2$ m^{-1}
$h = 44$ J/m^2 s K	$L_{ev} = 2.25 \times 10^6$ J/kg
$T_a = 300$ K	$T_{ev} = 373$ K
$h_f = 2$ m	$T_f = 1200$ K

h_f is the height of flame.

With $\beta = 2 \times 10^{-3}, \sigma = 400$ m$^{-1}, A = 5 \times 10^{-3}$ s^{-1}, $E = 1.398 \times 10^5$ J/mole, $R = 8.314$ J/mole K and $0 \leqslant V \leqslant 10$ m s^{-1}, we obtain $C_w = 1.74, A = 20, h = 0.28, v_r = 0.79, P_{ext} = 0.1, T_{ev} = 0.24, L_{ev} = 3.12$, and $0 < v_g < 2.27$.

We have used an explicit Euler algorithm in time. In the following simulations we will test the effect of wind, slope and humidity.

If we consider a ground vegetation (the area occupied by vegetation) density of $d = 0.5$, there is no wind and slope, we obtain a circular front fire as it is foreseen. The radius and the area of the burnt surface are plotted on Figs. 4–6.

If we consider a fire with wind for low value of the wind velocity the shape is elliptical. But when the wind is increased the shape does not remain elliptical (see also Fig. 7):

This shape is similar to the one which can be observed experimentally.

We can now consider the effect of the slope on the propagation. Let us consider a fire ignited between two hills:

One can see Fig. 8, the effect of slope on the fire. Along a slope the fire climbs faster and the top of the hill can be isolated.
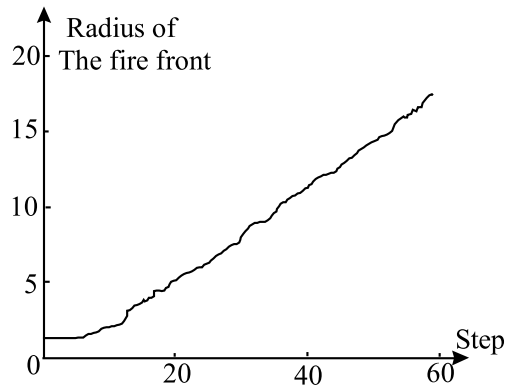

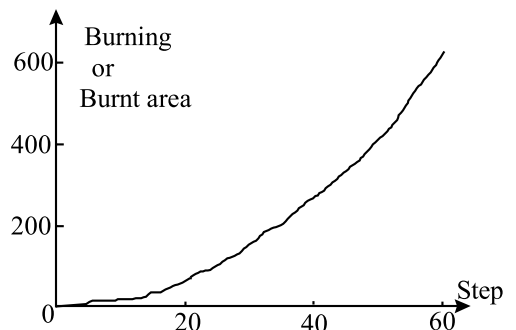Fig. 5. Evolution of the radius and the burning surface.

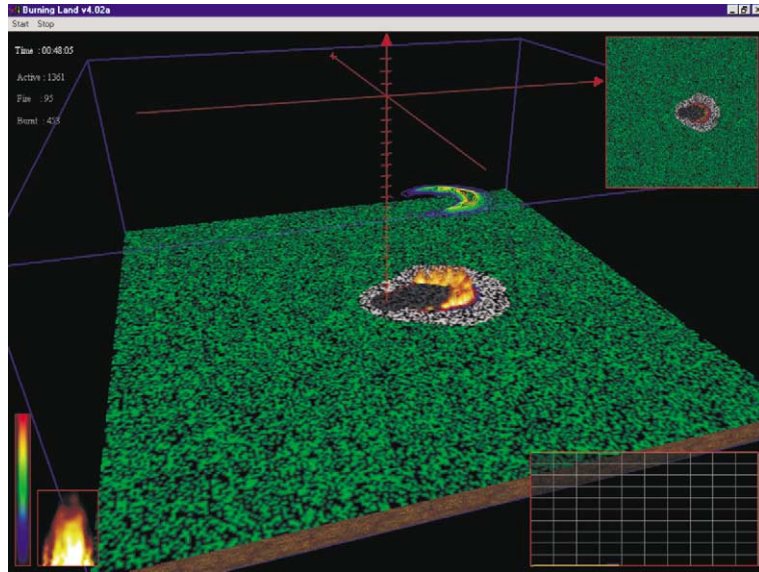Fig. 6. Evolution of the radius and the burning surface.
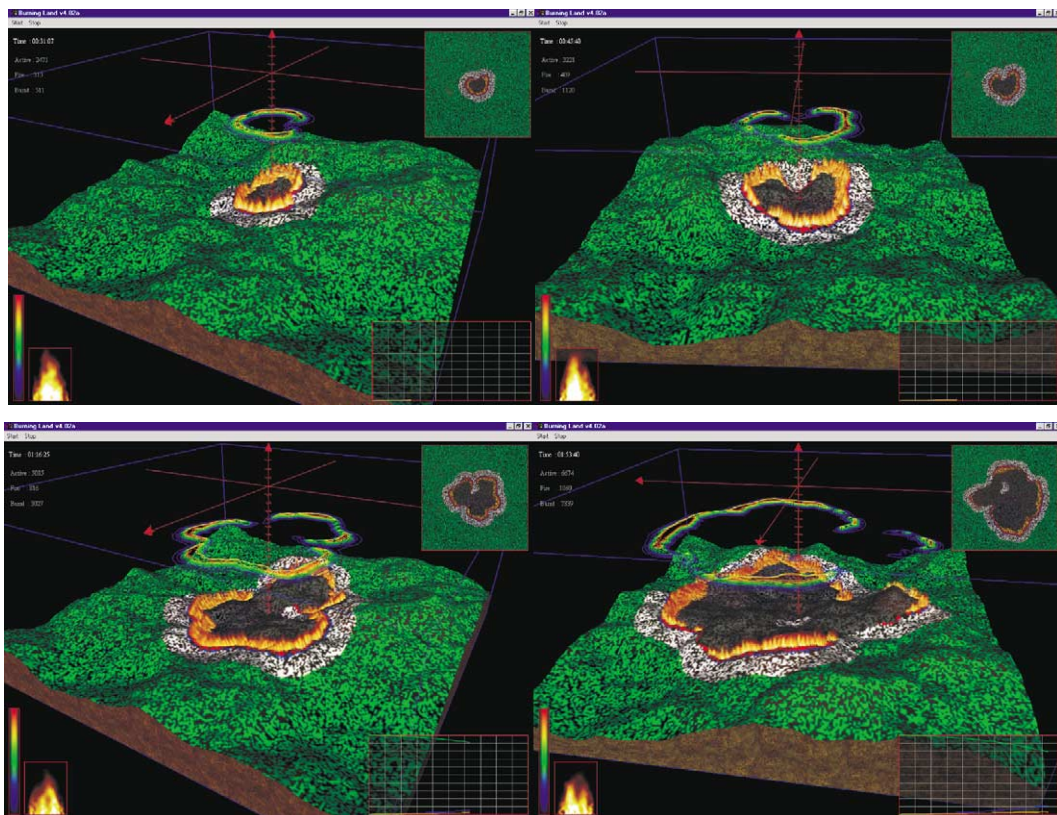
Fig. 7. Evolution of a fire with wind.

Fig. 8. Evolution of a fire with slope.

5.2. Percolation density

We can study the influence of the vegetation density on the propagation in an homogeneous forest. If the density occupation is not sufficient the fire will not propagate. Therefore there is a threshold above this threshold the fire will propagate to infinity under this threshold it will extinguish. This phenomenon is similar

to the critical density in percolation theory. This critical density depends on the parameters of the simulation. For a height of flames providing an influence neighbourhood of 30 cells grid points in each direction and a humidity of 7% we obtained for example a critical density of 0.34.

We can now plot this critical density as a function of the other parameters. As one can see in Fig. 9 there is an upper value for humidity. Above this value the fire will never propagate and it can be called extinction humidity.

Let us notice in Fig. 10 that near the critical density the fire front is no more circular, and posses some fractal structure. It means that the envelope model where the simulations are based on a normal velocity of the front should be inadequate in this range of parameters.

Of course other type of information can be provided as temperature or intensity of the fire, humidity and load.
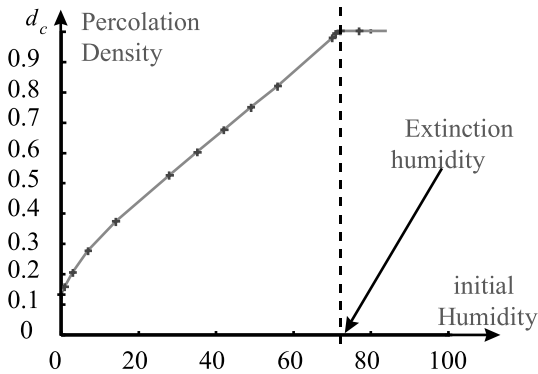

Fig. 9. Critical percolation density as a function of humidity.

6. Conclusion

In this paper we have seen that, with reasonable assumptions, models of propagation for forest fire can be obtained from combustion models of vegetation. By an asymptotic expansion, with the height of vegetation as small parameter we have obtained several possible two-dimensional models. As indicated, only the inner expansion has been provided, so that the results, although interesting are incomplete. The more complex model, denoted by model III is adapted for vegetation weakly compact where the gas flow plays a prominent role. This model provides velocity, temperatures and mass fraction as well, in the vegetal stratum. Model II is an intermediate model where the velocity of gas in the vegetal stratum is supposed to be known. Model I is a reaction diffusion model, very similar to the ones postulated previously and it is physically relevant. Then the link between the so-called physical models and the combustion models is obtained. The assumptions made for doing the asymptotic expansion are valid outside the flames, probably in a domain which can extend to a zone relatively close to the flame. In the burning zone the preceding expansion is no more valid and an other asymptotic analysis should be done (inside the vegetal stratum). In this new analysis the main component of velocity should be vertical and the dominant term in thermal equations should be the chemical heat source. A very similar problem has been treated comprehensively by Joulin [11] for the study of particle-laden gaseous flames. Among the three types of models cited, model I is the simplest and it has been simulated numerically neglecting the heat conductivity inside the vegetal
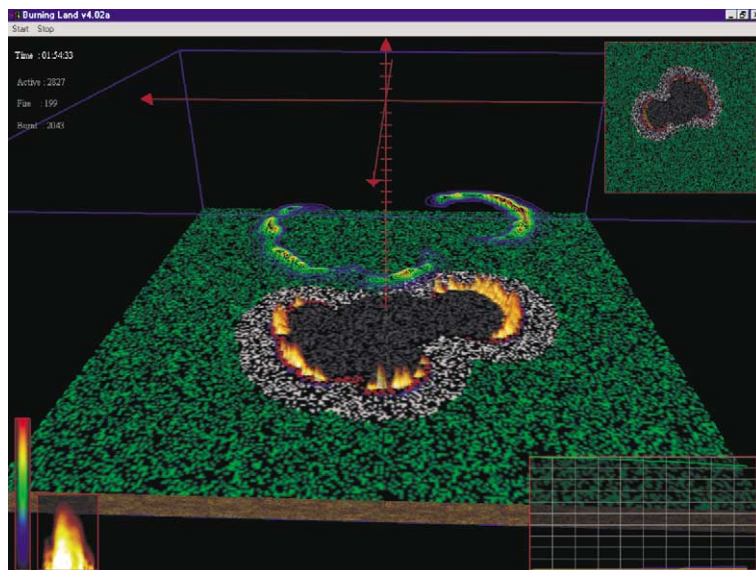

Fig. 10. Shape of the fire near the critical percolation density, $d = 0.35$.

stratum. This model is not really different from the one cited by Weber, that is Albini [2,3] and Catchpole et al. [4,7]. All these models differ only by the expression of the radiative term. The main contribution of this paper is to show that from a general model of combustion several models of propagation can be derived, and the one presented here is only a very particular one. In order to cope with wind and slope the radiant heat flux coming from the flame has been evaluated as a non-local convolution integral. And one can see that the estimation of the heat released by the flame is a crucial point for using these types of two-dimensional reaction diffusion models for determination of fire propagation. In the numerical simulations two free boundaries have been considered, the drying front and the pyrolysis front. Let us notice that the modelling of the drying and pyrolysis with sharp interfaces, as well as the dropping of heat conductivity has some advantages: the code is stable and fast. Real time simulations can be done in a PC.

Without a proper estimation of the radiant heat flux, two-dimensional simple reaction diffusion models, as model I, cannot pretend to simulate the propagation of fires. But in spite of their simplicity, they can provide good insight of the propagation of the front flame. For example the density of percolation, can give a significant index of danger provide it is evaluated for different heights of flames.

Appendix A. Derivation of the incident radiation M_r

It is impossible to give a closed form expression for the radiative flux without calculating the outer expansion of the asymptotic expansion. In this appendix we only estimate $M_r(M)$ at a point M in front of the burning domain that comes from the flame. The porous vegetal layer is assumed to be an absorbing–emitting grey medium. We assume that the flame is a perfect absorbing medium and that the gaseous phase out of the flame is a transparent medium so that heat fluxes $\mathbf{Q}_{fr}, \bar{\mathbf{Q}}_r$ are null out of the flame domain. The flux $\mathbf{Q}_{pr}$ is related to the radiative intensity L by the expression:

$$\mathbf{Q}_{pr}(\mathbf{x},t) = \int_{4\pi} L(\mathbf{x},\mathbf{u},t)\mathbf{u}\,d\Omega, \qquad (A.1)$$

where $d\Omega$ is the elementary solid angle in the direction $\mathbf{u}$.

The radiative intensity is supposed to satisfy the equation of transfer in an absorbing and emitting medium:

$$\nabla \cdot (L\mathbf{u}) = -KL + I, \qquad (A.2)$$

with K the extinction coefficient and $I(\mathbf{x},\mathbf{u},t)$ the source function given by:

$$I(\mathbf{x},\mathbf{u},t) = aL^0\big(T_p(\mathbf{x},t)\big)$$
$$+ \frac{\sigma_s}{4\pi}\int_{4\pi} L(\mathbf{x},\mathbf{u}',t)\Phi(\mathbf{x},\mathbf{u},\mathbf{u}')\,d\Omega'. \qquad (A.3)$$

with a the absorption coefficient, $\sigma_s = K - a$ the scattering coefficient. L^0 is the blackbody intensity $L^0[T_p] = B(T_p)^4/\pi$ and $\Phi(\mathbf{x},\mathbf{u},\mathbf{u}')$ the phase function for scattering. B is the Boltzmann number.

From relations (A.1)–(A.3) we derive by integration that the divergence of the flux $\mathbf{Q}_{pr}$ is given by

$$\nabla \cdot (\mathbf{Q}_{pr}(\mathbf{x},t)) = a(M)(4\pi L^0(T_p) - M(\mathbf{x},t)), \qquad (A.4)$$

where $M(\mathbf{x},t) = \int_{4\pi} L(\mathbf{x},\vec{\mathbf{u}},t)\,d\Omega$ is the incident radiation and L^0 is blackbody's intensity. From Albini [2], an isotropic repartition of convex particles leads to $a = \varepsilon_p(1-\Phi)\sigma/4$ and $\sigma_s = (1-\varepsilon_p)(1-\Phi)\sigma/4$, where ε_p is the solid porous emissivity and σ is particle surface to volume ratio.

We consider now a surface $\partial\mathcal{D}$ that surround the point M (cf. Fig. 11). Then if we assume that the vegetal phase is a blackbody, integration of (A.2) and (A.3) leads to

$$L(\mathbf{M},\mathbf{u},t) = L(0_{\mathbf{u}},\mathbf{u},t)\exp(-k(s))$$
$$+ \int_0^{k(s)} L^0[T_p(k',t)]$$
$$\times \exp\big[-(k(s)-k')\big]\,dk', \qquad (A.5)$$

where $k(s) = \int_0^s K(s')\,ds'$ and $s = \|\mathbf{O_uM}\|$ with $\mathbf{O_u}$ the intersection point of the radiative beam arising from $\mathbf{M} = \mathbf{x}$ in the direction $\mathbf{u}$ with the surface $\partial\mathcal{D}$. Surface and volume differential dS and dV are linked to differential solid angle $d\Omega$ by $dS = (\|\mathbf{MO_u}\|^2/\bar{\mathbf{n}}\cdot\bar{\mathbf{u}})\,d\Omega$ and $dV = \|\mathbf{MP}\|^2\,dk\,d\Omega/K(\mathbf{P})$ so that

$$M(\mathbf{M},t) = \int_{\substack{\partial\mathcal{D}\\ \text{visible from } M}} L(0_{\mathbf{u}},\mathbf{u},t)\xi(\mathbf{O_u},\mathbf{M})\mathbf{n}\cdot\mathbf{u}\,dS$$
$$+ \int_{\substack{\mathcal{D}\\ \text{visible from } M}} \Phi(\mathbf{P},t)\xi(\mathbf{P},\mathbf{M})\,dV, \qquad (A.6)$$

where $\Phi(\mathbf{P},t) = K(\mathbf{P})L^0[T_p(\mathbf{P},t)]$ and $\xi(\mathbf{P},\mathbf{M}) = \exp[-k(\|\mathbf{MP}\|)]/\|\mathbf{MP}\|^2$.

The blackbody assumption does not really change the radiation balance according to Albini study [2].

Incident radiation is the sum of two terms. The first one is related to boundary conditions and can be ne-
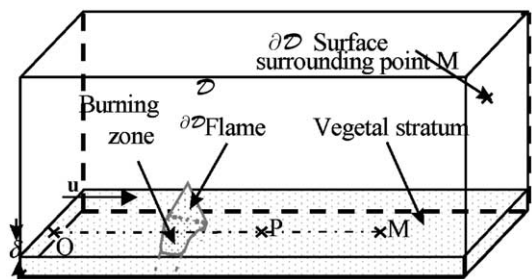

Fig. 11. Integration volume $\mathcal{D}$ and fire area

glected while the second is related to local emission at point **P** and to the attenuation through the beam from point **P** to point **M**. The second term is the sum of the radiation $M_f(\mathbf{M}, t)$ coming from the flame, radiation coming from outside the flame and from the local emission $4\pi K(\mathbf{M})L^0(T_p)$ around the point **M**. All terms a part from the flame radiation can be neglected, so that:

$$M(\mathbf{M}, t) = M_f(\mathbf{M}, t), \tag{A.7}$$

where

$$M_f(\mathbf{M}, t) = \int_{\Omega_f} \Phi(\mathbf{P}, t)\xi(\mathbf{P}, \mathbf{M})\,\mathrm{d}V \tag{A.8}$$

with Ω_f the domain occupied by the flames.

For calculating $M_f(\mathbf{M}, t)$ the integration runs on two sub-domains: the part Ω_{fp} in the vegetal stratum and the part Ω_{fa} above it. One can neglect this first integral and consider only the flame above the stratum. Now in the term $\xi(\mathbf{P}, \mathbf{M})$ of (A.8) we can choose $k(\|\mathbf{MP}\|) = K(\mathbf{P}\hat{MPD})\|\mathbf{MP}\|$ with the following anisotropic coefficient.

$$K(\mathbf{P}, \hat{MPD}) = K(\mathbf{P})\frac{(1 + \sin^2 \alpha_f)(1 - \sin \alpha_f \cos(\hat{MPD}))}{\cos^2 \alpha_f}, \tag{A.9}$$

where the flame is inclined to the normal to the floor plane by an angle α_f due to the wind, and $\hat{MPD}$ is the angle between the inclined flame direction and the segment $[PM)$. The inclined flame direction is the local wind direction. Here, the the anisotropic length of attenuation are choose elliptical. This relation is similar to Dorrer [8] anisotropic extinction coefficient but Dorrer choose elliptical extinction coefficient instead of elliptical length of attenuation but there is no rigorous proof.

Now, the above three-dimensional relations (A.7)–(A.9) should be reduced to a two-dimensional one on the forest strata plane $\mathcal{S}$ that can be locally considered as an inclined plane (cf. Fig. 12). We assume that $\delta \ll L, h_f = \mathrm{O}(\delta)$ and $1/K = \mathrm{O}(\delta)$.

Let Ω_f^s be the fire domain on the plane $\mathcal{S}$. Then we consider a point M, on the plane $\mathcal{S}$, in front of the fire domain and a point P, on the plane $\mathcal{S}$, into the fire domain. Let φ the angle between the segment $[P, M]$ and the line of highest slope **p** at point P. The line **p** is directed by the vector **k**. Let **n** be the normal to the plane $\mathcal{S}$ at point P and $\mathbf{k}^\perp$ the orthogonal vector to **k** and **n**. The flame shape at point P is defined by the straight line **D** and by its height h_f. This height is supposed to be known. Then let **d** be the projection of **D** onto the plane $\mathcal{S}$. The direction of **D** is given by the two angles α_f and φ_f (cf. Fig. 12).

From relation (A.8) one obtains by projection

$$M_r(\mathbf{M}, t) = \delta M(\mathbf{M}, t) = \int_{\Omega_f^s} \varphi(\mathbf{P}, t)\xi(\mathbf{P}, \mathbf{M})\,\mathrm{d}S \tag{A.10}$$
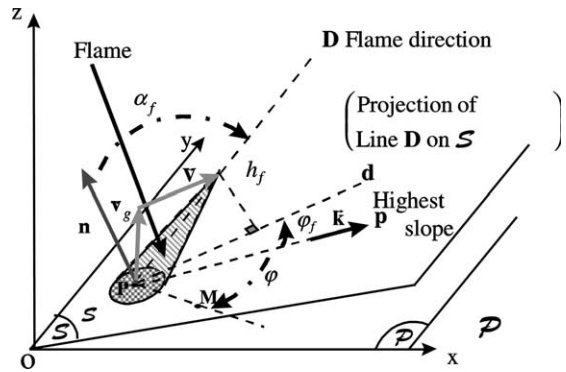

Fig. 12. Shape of the flame.

with

$$\xi(\mathbf{P}, \mathbf{M}) = \frac{K(\mathbf{P})}{\|\mathbf{MP}\|}$$
$$\times \exp\left(-K(\mathbf{P})\frac{(1 + \sin^2 \alpha_f)(1 - \sin \alpha_f \cos(\varphi - \varphi_f))}{\cos^2 \alpha_f}\|\mathbf{MP}\|\right) \tag{A.11}$$

and

$$\varphi(\mathbf{P}, t) = \delta h_f K(\mathbf{P})T^4(\mathbf{P}, t). \tag{A.12}$$

Relations (A.10)–(A.12) are relations (37)–(39) for the incident radiation $M_r(\mathbf{M})$. Note that we use a projection of incident radiation to obtain the two-dimensional incident radiation. This is not a rigorous proof but it leads to the interesting above isotropic two-dimensional incident radiation.

References

[1] G. Albinet, G. Searby, D. Stauffer, Fire propagation in a 2-D random medium, J. Phys. 47 (1986) 1–7.

[2] F.A. Albini, A model for fire spread in wildland fuels radiation, Combust. Sci. Technol. 42 (1985) 229–258.

[3] F.A. Albini, Wildland fire spread by radiation: a model including fuel cooling by convection, Combust. Sci. Technol. 45 (1985) 101–113.

[4] D.H. Anderson, E.A. Catchpole, N.J. De Mestre, T. Parkes, Modelling the spread of grassland fires, J. Austral. Math. Soc. (Series B) 13 (1982) 452–466.

[5] J.C.S. Andre, D.X. Viegas, A strategy to model the average fireline movement of a light to medium intensity surface forest fire, in: Proceedings of the Second International Conference on Forest Fire Research, Coimbra, Portugal, vol. 1, 1994, pp. 221–242.

[6] T. Beer, Percolation theory and fire spread, Combust. Sci. Technol. 72 (1990) 297–304.

[7] E.A. Catchpole, M.E. Alexander, A.M. Gill, Elliptical-fire perimeter- and area-intensity distributions, Can. J. For. Res. 22 (1992) 968–972.

[8] G.A. Dorrer, A model for propagation of curvilinear forest fire fronts, Krasnoyarsk, Fizika Goreniya i Vzryva 20 (1984) 11–19 (translated).

[9] J.A.M.S. Duarte, Fire spreading in natural fuels: a computational aspect, Ann. Rev. Comput. Phys. V (1997) 1–23.

[10] A.M. Grishin, in: F. Albini (Ed.), Mathematical Modeling of Forest Fires and New Methods of Fighting Them, 1997 (translated by M. Czuma, L. Chikina, L. Smokotina).

[11] G. Joulin, Temperature-lags and radiative transfer in particle-laden gaseous flames. Part I: steady planar fronts, Combust. Sci. Technol. 52 (1987) 377–395.

[12] M. Larini, F. Giroud, B. Porterie, J.C. Loraud, A multiphase formulation for fire propagation in heterogeneous combustible media, Int. J. Heat Mass Transfer 41 (1998) 881.

[13] W.K. Mossner, B. Drossel, F. Schwabl, Computer simulations of forest-fire model, Phys. A 190 (1992) 205–217.

[14] T. Ohtsuki, T. Keyes, Biased percolation: forest fires with wind, J. Phys. A 19 (1986) L281–L287.

[15] N. Provatas, T. Ala-Nissila, M. Grant, K.R. Elder, L. Piché, Scaling, propagation and kinetic roughening of flame fronts in random media, J. Statist. Phys. 81 (1995) 737–759.

[16] G.D. Richards, An elliptical growth model of forest fire fronts and its numerical solution, Int. J. Numer. Meth. Eng. 30 (1990) 1163.

[17] G.D. Richards, A general mathematical framework for modelling two-dimensional wildland fire spread, Int. J. Wildland Fire 5 (1995) 63–72.

[18] G.D. Richards, W. Bryce, A computer algorithm for simulating the spread of wildland fire perimeters for heterogeneous fuel and meteorological conditions, Int. J. Wildland Fire 5 (1995) 73–79.

[19] R.C.Rothermel, A mathematical model for predicting fire spread in wildland fuels, USDA Forest Service Research paper INT-115, Ogden, UT, USA, 1972, p. 40.

[20] O. Séro-Guillaume, J. Margerit, Modelling forest fires. Part I: a complete set of equations derived by extended irreversible thermodynamics, Int. J. Heat Mass Transfer 45 (2002) 1705–1722.

[21] C.E. Van Wagner, A simple fire-growth model, Forestry Chron. 45 (1969) 103–104.

[22] W. Von Niessen, A. Blumen, Dynamic simulation of forest fires, Can. J. For. Res. 18 (1988) 805–812.

[23] G. Wallace, A numerical fire simulation model, Int. J. Wildland Fire 3 (1993) 111–116.

[24] R.O. Weber, Analytical models for fire spread due to radiation, Combust. Flame 78 (1989) 398–408.

[25] R.O. Weber, Toward a comprehensive wildfire spread model, Int. J. Wildland Fire 1 (1991) 245–248.

[26] R.O. Weber, Modelling fire spread through fuel beds, Progr. Energy Combust. Sci. 17 (1991) 67–82.